State-of-the-Art Renal Imaging in Children

Bernarda Viteri, MD,[a,b,c] Juan S. Calle-Toro, MD,[b] Susan Furth, MD,[a,c] Kassa Darge, MD,[b,c] Erum A. Hartung, MD,[a,c] Hansel Otero, MD[b,c]

abstract

Imaging modalities for diagnosing kidney and urinary tract disorders in children have developed rapidly over the last decade largely because of advancement of modern technology. General pediatricians and neonatologists are often the front line in detecting renal anomalies. There is a lack of knowledge of the applicability, indications, and nephrotoxic risks of novel renal imaging modalities. Here we describe the clinical impact of congenital anomalies of the kidneys and urinary tract and describe pediatric-specific renal imaging techniques by providing a practical guideline for the diagnosis of kidney and urinary tract disorders.

Renal imaging continues to evolve rapidly. From advances in conventional kidney ultrasound to quantitative imaging evaluation, new technologies are transforming how we assess kidney function and disease. Congenital anomalies of the kidney and urinary tract (CAKUT) are the most common cause of end-stage renal disease in children and, consequently, the most common cause of the need for renal replacement therapy, such as dialysis, in this patient population.[1,2] As a result, imaging is crucial for early detection of kidney and urinary tract disease, monitoring of kidney function, and enhancing the assessment of disease progression and prognosis. Conventional methods for the diagnosis of renal dysfunction based on clinical chemistry measurements (such as serum creatinine level) have been shown to be suboptimal for early detection of functional loss.[3]

CAKUT includes a variety of disorders that arise during the development of the kidneys, ureters, bladder, and urethra in fetal life. Although CAKUT tends to present sporadically, associated anomalies have been described in up to 30% of infants born with CAKUT.[4] CAKUT constitutes 20% to 30% of all anomalies identified in the prenatal period and occurs in up to 60% of children with chronic kidney disease (CKD) in the postnatal period.[1,2,5] Common types of CAKUT result from failure of normal nephron development (renal dysplasia, renal agenesis, and multicystic renal diseases), abnormalities of embryonic migration of the kidneys (ectopic kidneys and horseshoe kidneys), and abnormalities of the developing urinary collecting system (vesicoureteral reflux [VUR], ureteropelvic junction obstruction, lower urinary tract obstruction, etc). CAKUT often presents with urinary tract dilation (UTD), previously referred to as hydronephrosis.[6,7]

Although hydronephrosis remains a commonly used term, it often has different meanings among practitioners. In 2014, a unified consensus reached among multiple professional societies recommended replacing the term hydronephrosis with the more specific descriptor UTD to denote an imaging finding in a system that may or may not be under pressure (ie, obstructive versus nonobstructive

STATE-OF-THE-ART REVIEW ARTICLE

UTD).[8] Antenatal and postnatal UTD each have their own scoring system for reference (Fig 1).[8] Higher scores relate to a higher degree of dilatation and renal parenchymal, ureteral, and/or bladder abnormalities that require further workup and monitoring.[9]

There is currently no single gold standard to assess obstructive uropathy in children, and usually, a combination of imaging tests are used.[10–12] Although renal bladder ultrasound, fluoroscopy, and nuclear medicine functional studies remain the main tools for anatomic and functional diagnosis and management of UTD and CAKUT, novel technologies have been added to the armamentarium of pediatric renal imaging. Emerging technologies that are increasingly being used in clinical settings include functional magnetic resonance urography (fMRU), contrast-enhanced ultrasound (CEUS), and contrast-enhanced voiding ultrasound, which can delineate anatomy at a higher resolution and provide functional, perfusion, and excretion information of the kidneys and urinary tract without using ionizing radiation. Additional techniques that remain under study include three-dimensional (3D) printing, elastography, and volumetric analysis. Our purpose for this article is to provide a comprehensive overview of renal imaging modalities with an emphasis on novel techniques and their potential clinical value in the detection and monitoring of children with kidney disease.

ANATOMIC IMAGING

Ultrasound

Renal and bladder ultrasound (RBUS) is the first-line imaging modality for evaluation of the renal anatomy in children because it is noninvasive, is broadly available, is relatively fast, lacks ionizing radiation, and is less costly than other imaging modalities. Additionally, ultrasound does not require specific patient positioning or the need to be in a machine, which allows for imaging of children while in supine, prone, semi-upright or upright positions or, in the case of infants, while being held by a caregiver. RBUS depicts kidney size (and growth over time), echogenicity, echotexture, parenchymal thickness, the duplex system, and the degree of dilatation of the pelvocalyceal system and ureters in children.[13] RBUS can be used to identify masses and large calculi, can be used to measure pre- and postvoid bladder volumes, and can provide real-time images for guidance of interventional procedures.

During basic ultrasound imaging, the kidney may be divided into an outer cortex and an inner medulla. The cortex is composed of an outer rim of tissue as well as columns of cortical tissue that descend between the medullary pyramids (Fig 2A). These columns have been termed the septal cortex, also commonly referred to as columns of Bertin (Fig 3). The medulla is composed of a variable number of renal pyramids, with the base of the pyramid formed by its overlying renal cortex and its apex by the renal papilla that projects into a minor calyx. The papillae are cone-shaped structures that contain the openings of the collecting ducts, which empty into the calyces. A calyx
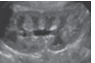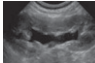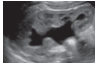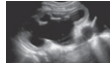
	Normal	UTD P1	UTD P2	UTD P3
AP renal pelvis diameter	<10 mm	≥10-15 mm	≥15 mm	≥15 mm
Calyceal dilation	None	Central only	Peripheral	±Central and/or calyceal[a]
Parenchymal thickness	Normal	Normal	Normal	Abnormal
Parenchymal appearance	Normal	Normal	Normal	Abnormal
Ureters	Normal	Normal	Abnormal	± Normal or abnormal[a]
Bladder/Urethra	Normal	Normal	Normal	Abnormal
		Recommendations		
Renal/Bladder Ultrasound	No	1-6 months	1-3 months	1 month
VCUG/CeVUS	No	At discretion of physician	At discretion of urologist/nephrologist (recommended If abnormal ureters)	Recommended
MAG-3/ fMRU	No	No	At discretion of urologist/nephrologist (to rule out upper tract obstruction)	Recommended

FIGURE 1
Postnatal UTD classification and recommendations with grayscale ultrasound representative examples. Postnatal presentation for UTD P1, low risk; UTD P2, intermediate risk; UTD P3, high risk. Classification is based on the most significant ultrasound finding. For example, if the anterior-posterior renal pelvis diameter is found within UTD P1 range, but there is peripheral calyceal dilation, then the correct classification is UTD P2. [a] Calyceal dilation and ureteral dilation are often present in patients with UTD P3 but are not needed to qualify for UTD P3 if there is UTD with either abnormal parenchymal thickness, abnormal parenchymal appearance, or abnormal bladder. Adapted from Nguyen HT, Benson CB, Bromley B, et al. Multidisciplinary consensus on the classification of prenatal and postnatal urinary tract dilation (UTD classification system). J *Pediatr Urol.* 2014;10(6):982–998 and Chow JS, Koning JL, Back SJ, Nguyen HT, Phelps A, Darge K. Classification of pediatric urinary tract dilation: the new language. *Pediatr Radiol.* 2017;47(9):1109–1115.
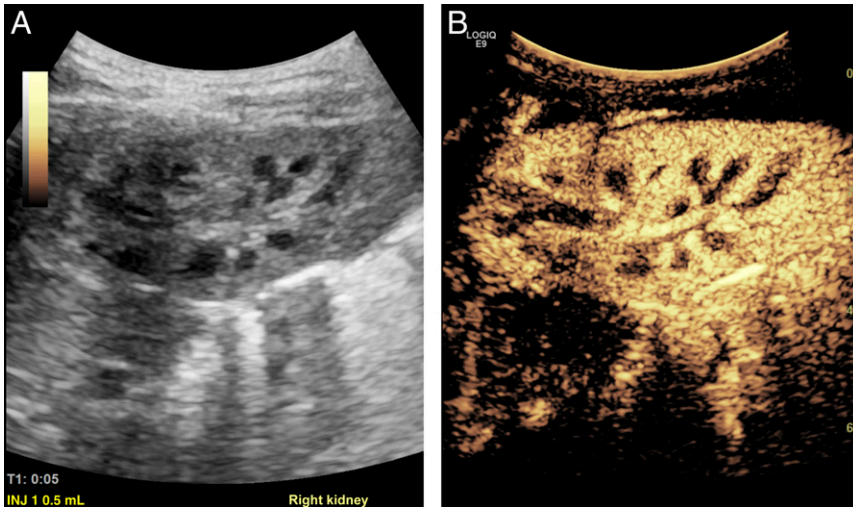
FIGURE 2
A and B, Normal renal anatomy of the right kidney as seen on sagittal grayscale and CEUS in a 13-month-old girl with febrile UTI.

is a cup-shaped portion of the intrarenal collecting system. The calyces, infundibula, and renal pelvis are jointly referred to as the intrarenal collecting system.[14]

Emerging Ultrasound Technologies

Three-Dimensional Ultrasound and Ultrasound Elastography

Novel technologies can now provide 3D images with higher spatial and contrast resolutions compared with previous 3D modalities.[15] Clearer and sharper ultrasound images (with fewer artifacts) allow accurate reconstructive analysis of the anatomy (Fig 4), better tissue differentiation (eg, fluid-filled structures), and improved identification of echo-enhancing structures, such as renal stones and renal parenchymal lesions.[16,17] One has to be cautious in interpreting higher-resolution images, however, because the corticomedullary differentiation can be overly enhanced and may falsely mimic nephrocalcinosis.[18]

Three-dimensional ultrasound (3DUS) provides volumetric evaluation and more complete visualization of the collecting system, and it decreases imaging time by requiring a single sweep with reconstruction in multiple planes at a later time.[19,20] Therefore, interest now lies in supporting quantitative imaging analysis, such as automated segmentation of the kidneys and urinary tract, to enhance the care of children with UTD.

Given parenchymal volume calculations from 3DUS are comparable to those from dimercaptosuccinic acid scintigraphy and magnetic resonance urography (MRU), its emergence can result in decreased use of computed tomography (CT), MRI, and diuretic renography.[21,22] Similarly, high-quality 3DUS depiction and segmentation of the collecting system, which may have the potential to better reveal complex anatomy, may result in decreased need for fluoroscopic evaluation of the collecting system or MRU. Additionally, 3DUS provides a multiaxial demonstration of the entire kidney.[15,16]

Shear-wave elastography is another advance in ultrasound technology that is a noninvasive way to assess tissue stiffness.[23,24] The ultrasound transducer sends an acoustic wave into the tissue to create a wave of tissue displacement. Tissue stiffness derives from the speed at which the displacement wave traverses the
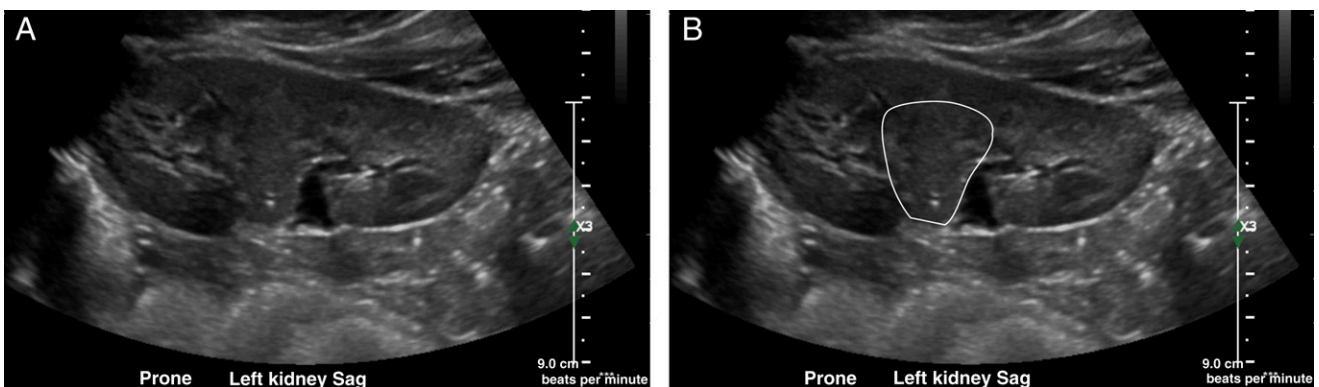

FIGURE 3
A, Grayscale ultrasound in an 8-year-old girl with day wetting reveals a normal left kidney with a prominent column of Bertin, which is a common normal variant that could be mistaken for a lesion (renal pseudotumor) because, as delineated in B, it interrupts or splits the normal renal sinus. Sag, sagittal.
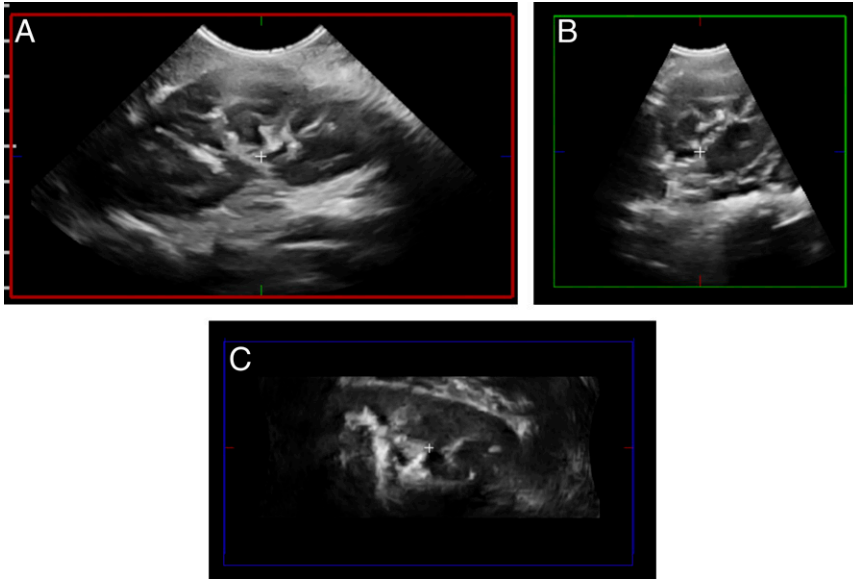
FIGURE 4
3DUS scanning of the left kidney. A, After a single automatic "sweep" in the sagittal plane (red box). B and C, Additional axial (green box) and coronal (blue box) images can be reconstructed from the original sagittal images in this 7-year-old girl with a right renal mass (not shown).

tissue, as measured by a second ultrasound pulse (Fig 5). This modality has been more broadly studied in the liver (eg, to measure fibrosis in autosomal-recessive polycystic kidney disease), thyroid, breast, gastrointestinal tract, and prostate.[23,25] More recently, elastography has been investigated in the kidney to measure fibrosis and changes in tissue stiffness in CKD, kidney allografts, and VUR. Further characterization of focal renal lesions is another applicability in which elastography is being studied.[26]

New two-dimensional ultrasound technologies now include semiautomatic quantification of UTD severity.[27] For this, postprocessing imaging software uses the ultrasound data to calculate multiple parameters, such as size of the collecting system, depth of calyces, thickness of parenchyma, geometric shape, circularity ratio, and curve descriptors. An algorithm then uses these measurements to identify those patients who will benefit from renal function tests (ie, diuretic renography), saving the inconvenience, risks, and nonrequired ionizing radiation of additional testing on those who do not meet criteria.[27]

CEUS

CEUS is an innovative imaging modality that uses nonnephrotoxic microbubbles (gas core with a lipid monolayer stabilizing shell no bigger than a red blood cell) as an intravenous (IV) ultrasound contrast agent (UCA), as seen in Fig 2B. UCAs are currently approved by the US Food and Drug Administration for IV use in cardiac and hepatic ultrasounds and for intravesical use for the evaluation of VUR in children. Despite being off label in the United States, its renal applications have grown in recent years.[28] CEUS has been shown to be more sensitive in detecting perfusion abnormalities than Doppler (Fig 6). This is due to the ability of CEUS to enhance the vascular echo signal through the use of a purely intravascular contrast agent rather than by detecting the Doppler shift, which is highly dependent on many technical factors, such as speed of acquisition, angle of imaging, depth of imaging, and frequency.[29] CEUS in clinical practice provides dynamic information, such
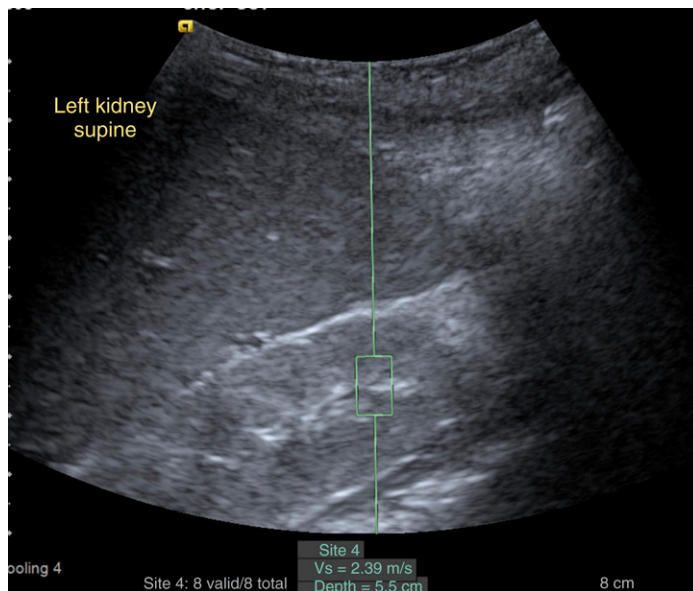

FIGURE 5
Ultrasound shear-wave elastography of the left kidney in a 3-year-old with cerebellar vermis hypo/aplasia, oligophrenia (mental retardation), ataxia, ocular coloboma, and hepatic fibrosis syndrome reveals normal renal stiffness (velocity 2.39 m/second). The elastography samples the tissue inside the box, and its value is expressed as the velocity of the wave through the tissue (Vs) (ie, measuring the velocity of a vibration wave generated from the probe on the skin of the patient).
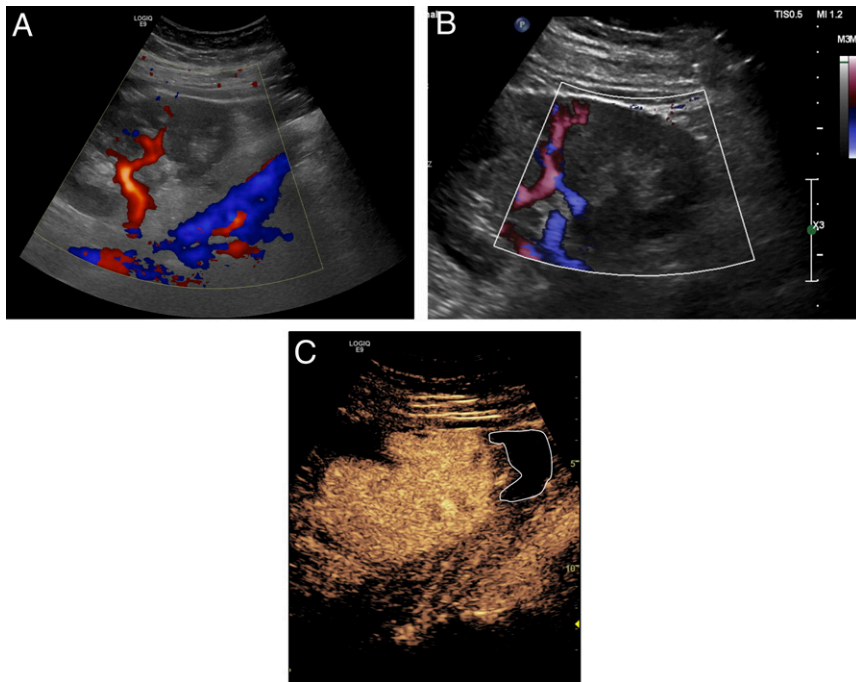
FIGURE 6
Ultrasound images on day 2 after right lower-quadrant transplant of allograft kidney in a 15-year-old girl revealing hypoperfusion to lower pole. A, Color Doppler. B, Power Doppler. C, CEUS (white delineation highlights hypoperfused lower pole region).

as perfusion of the microvasculature of the kidney and, potentially, the quantification of renal blood flow as well as additional perfusion characteristics of masses and cystic lesions.[30–32] In kidney transplantation, CEUS has been able to detect early features of allograft dysfunction in the setting of acute tubular necrosis, rejection, cortical necrosis, and other vascular complications.[33–35] A small-sample adult study revealed that CEUS might be a good prognostic marker reflecting microvascular characteristics of the kidney allograft itself, independent of the vasculature of the recipient.[36] Consequently, it may be a nonimmunologic predictor of long-term kidney allograft function.

Performance of CEUS usually involves at least 2 people: the scanner operator in charge of image acquisition and a second member (eg, nurse, sonographer, or radiologist) responsible for the contrast IV administration. With a single

injection, one can obtain images of a lesion or region of interest, 1 (Fig 2B) or both kidneys. Repeating the initial dose 1 time will allow one to obtain "first-pass" images for each kidney separately. First-pass images represent the initial contrast flow from the arteries into the renal cortex and, subsequently, the parenchyma as opposed to equilibrium or washout images, which refer to later images in which the contrast diffuses into the pyramids and later reabsorbs. Postacquisition quantification of perfusion or relative enhancement is, to date, a work in progress with no standardization but promising preliminary results.[37,38]

Voiding Cystourethrography

Fluoroscopic voiding cystourethrography (VCUG) is the gold standard for diagnosing and grading VUR and is used to evaluate the bladder and urethra in detail as well. VUR is suspected on the basis of UTD, ureteral dilatation, an abnormal

RBUS (such as uroepithelial thickening or scarring) after first febrile urinary tract infection (UTI), recurrent UTI, dysfunctional voiding (such as neurogenic dysfunction of the bladder), and bladder outlet obstruction, among others. It is important to note that in some circumstances, a retrograde urethrogram, in which only the urethra is imaged, may be preferred over a VCUG, particularly in children with trauma or dysuria. By using a bladder catheter, iodinated contrast material is instilled into the bladder, and pulsed fluoroscopy, the last image held, or the fluoroscopic screen capture (which results in a much lower radiation dose) is obtained. Key images are as follows: (1) an early-filling, last-image capture of the bladder, which may reveal an intravesical ureterocele or other masses; (2) early oblique views; (3) oblique radiographs of the bladder at full capacity before voiding; (4) images of the urethra during voiding before and after removal of the catheter (lateral for male patients and frontal for female patients); and (5) images of the renal fossae immediately after voiding to document the presence and grade of reflux or its absence. Cyclical filling of the bladder (filling to capacity followed by voiding and refilling for a second or third time) is helpful in infants (1 year of age or younger) who void at low volumes.[39]

Contrast-Enhanced Voiding Urosonography

Contrast-enhanced voiding urosonography (CeVUS) is an ultrasound-based, radiation-free alternative to evaluate for VUR or urethral pathology.[40,41] CeVUS uses an UCA, and, like in VCUG, the contrast is administered via a bladder catheter. When compared with VCUG (Fig 7), CeVUS has been shown to be more sensitive in detecting VUR, with a higher grade of reflux in up to two-thirds of patients, and has been shown to be as good for the
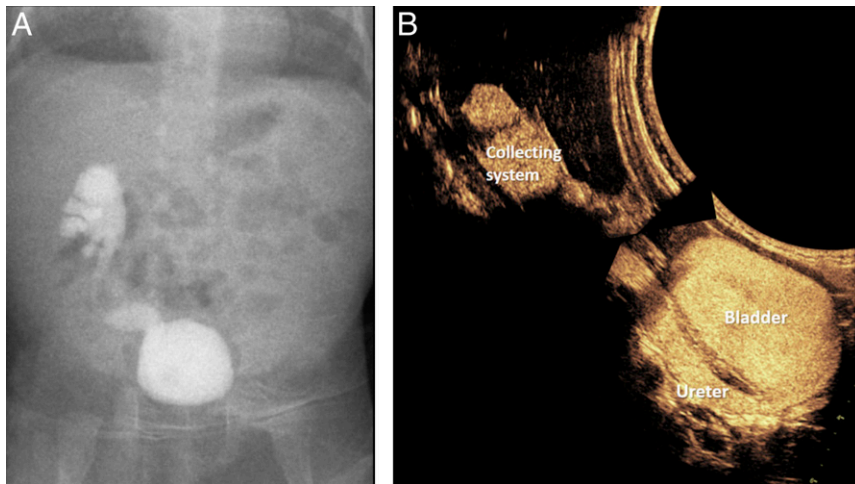
FIGURE 7
A and B, Right grade 4 VUR on a 1-month-old girl on VCUG without significant interval change, compared with CeVUS (image reconstructed to ease comparison) at 2 years of age.

evaluation of the urethra.[42,43] CeVUS is performed by using an ultrasound scanner, which is smaller and more pediatric friendly than a fluoroscopy suite. It can be performed in different positions (eg, scanned from the back while sitting or standing) while caregivers are holding their children or are nearby. Similar to VCUG, the bladder is filled under ultrasound monitoring, followed by alternate scanning of the right and left kidneys and the bladder. During voiding, additional urethral suprapubic and/or transperineal scans are performed with the catheter in place, and after catheter removal, additional postvoid scans are performed. The detection of microbubbles within a ureter or renal collecting system indicates VUR, which is graded similarly in VCUG.[44] As with VCUG, cyclical filling may be necessary in neonates and infants. UCAs have a good safety profile for intravesical use, with no known side effects.[40]

CeVUS involves 2 team members with similar tasks, as described for CEUS performance (see previous section); however, similar to VCUG, the supervising radiologist remains in the room during the entire procedure. CeVUS has the potential of replacing some of the clinically indicated VCUG and will be incorporated as an equivalent test with the same indications in the 2019 revision of the American College of Radiology–Society of Pediatric Radiology Practice Parameter for the Performance of Voiding Cystourethrography in Children (K.D., personal communication, 2019). Moreover, in therapeutics, intraoperative applicability of CeVUS has improved Deflux injection success rates, with increased resolution of VUR by ~20%.[45]

3D Printing

In 2013, the Radiologic Society of North America launched a program on 3D printing that included the fabrication of organs as depicted on CT and magnetic resonance (MR) images, which included an excellent delineation of kidney morphology. Since its introduction, newer 3D printing formats have been developed to incorporate surface texture, color, and material properties into the models.[46] These 3D-printed models are patient specific and serve as innovative presurgical and preintervention tools. In renal disease, 3D models have revealed high accuracy in replicating complex anatomic structures and pathologies.[47,48] Models of the kidneys with renal tumors have been reported to enhance the understanding of surgeons, trainees, and patients and their families regarding the goals of surgery.[46–51] This has generated an improvement in patient education and satisfaction.[51] As surgical approaches evolve from traditional open to minimally invasive approaches, 3D printing becomes an increasingly valuable surgical planning and simulation tool.[49,52,53] As the technology expands and becomes more broadly available, it may become standard of care, especially in complex anatomic cases.

CT

CT allows for high anatomic definition and provides a panoramic image of the kidney and urinary tract. It is a fast and volumetric (ie, the size of pixels is similar in all planes, and hence pixels are commonly referred to as "voxels") imaging modality that allows for 3D and multiplanar reconstructions in all planes. Postprocessing can use the raw data as the base for 3D-printed models. CT is the main imaging modality for evaluating renal pathology in adults but is less preferred in pediatrics because of lower incidence of stones and malignancies in children and to avoid ionizing radiation exposure.[54,55] In children, CT without contrast is the recommended imaging modality for evaluation of suspected urolithiasis after an equivocal ultrasound for treatment planning of known cases of urinary stones and in traumatic hematuria.[56] CT angiography is used to evaluate suspected renovascular hypertension as an alternative to Doppler ultrasound or MR angiography (Fig 8). When a contrast-excretion phase is included in the CT examination, it is called CT urography (Fig 9), which is

FIGURE 8
Bilateral renal artery stenosis in a 4-year-old with systolic blood pressures in the 200s who was subsequently diagnosed with fibromuscular hyperplasia. A and B, CT images and angiography reveal long-segment severe stenosis of the right renal artery near the aortic origin and a shorter segment of severe stenosis on the left, both sides with poststenotic dilatation.

useful in the evaluation of trauma, suspected urinary tract obstruction, or calyceal diverticula.[57] Although CT IV iodinated contrast agents are generally safe, there is a possible risk of postcontrast acute kidney injury (PC-AKI).[58–60] PC-AKI incidence was reported at 10% in a small cohort of children.[61] However, PC-AKI is a correlative diagnosis that has been challenged more recently.[62] The association, or lack thereof, between CT iodinated contrast administration and PC-AKI in children is yet to be established; moreover, a newer generation of CT scanners allows for lower radiation doses.

FUNCTIONAL IMAGING

Functional Renogram

Nuclear medicine functional renal scans follow the uptake and excretion of radiotracers, also called radiopharmaceutical agents, through the kidneys and into the collecting system. Unlike other imaging modalities that rely on an external radiograph source, nuclear medicine scanners capture γ-rays emitted from the patient's body after radiotracer administration, hence reflecting the distribution of radiotracers in the patient and expressed in counts over time. Some variations in the nomenclature and protocol exist, and

these studies are also referred to as furosemide renography, renal scintigraphy, radionuclide renal scintigraphy, diuretic renography, radioisotope renography, and nuclear medicine renogram. The study can be completed by using different radiotracers classified by their uptake and clearance mechanisms as agents for glomerular filtration (^{99m}Tc-labeled diethylenetriaminepentaacetic acid [DTPA]), tubular secretion (^{99m}Tc-labeled mercaptoacetyltriglycine [^{99m}Tc-MAG3]), or cortical tubular binding (^{99m}Tc-labeled dimercaptosuccinic acid [^{99m}Tc-DMSA]).[10,63–65]

In the dynamic function of renal scans, the renal blood flow is first evaluated immediately after IV injection of the radiotracer bolus, after the first pass of the tracer to the kidney. Then the uptake and clearance function are assessed over the next 20 to 30 minutes in 10- to 20-second frames.[10,65] When incomplete radiotracer drainage leads to concern of urinary tract obstruction, a loop diuretic is given and a second series of images is acquired for an additional 20 to 30 minutes while the bladder empties. These images help calculate a filtration rate that provides information regarding how well the

FIGURE 9
Normal renal anatomy as seen in CT urography in a 14-year-old boy. A, Coronal noncontrast CT image reveals the outline of the kidneys and is useful in identifying stones and calcifications (when present). B, Coronal CT postcontrast image by using a split-bolus technique (which allows for the evaluation of the renal cortex and collecting system in a single set of images) reveals the normal enhancement of the cortex as well as the contrast within the collecting system, properly delineating the calyces (yellow arrow) and renal pelvis (magenta star).

kidney is functioning and if there is an obstruction.[65] These images are used to calculate the clearance rate of the radiotracer, which is measured as washout half-time. In patients with difficulty emptying the bladder, such as infants, or patients with neurogenic bladder, placement of a urinary catheter is recommended before initiation of the study so that results can be analyzed in an otherwise unobstructed outlet system.[10,65] It is important to note the residual urine volume can be measured as pre- and postvoid bladder counts.[66]

Mercaptoacetyltriglycine and DTPA are rapidly taken up by the kidney via different mechanisms and later excreted via the urinary tract. DTPA is freely filtered by glomeruli and is not secreted or reabsorbed by the tubules before being excreted. Hence, it can be used to measure the glomerular filtration rate by quantifying the amount of filtrate formed per minute.[10,63,64] Mercaptoacetyltriglycine is not filtered through the glomerular membrane, and its extraction requires delivery of the compound to the kidney (renal plasma flow) and extraction from the plasma (renal tubules). Hence, clearance of mercaptoacetyltriglycine is expressed as the effective renal plasma flow, an approximation of renal plasma flow (unadjusted by specific extraction and filtration factors) (Fig 10).[67] ^{99m}Tc-DMSA binds to the cortical tubules, and it remains in the renal parenchyma for an extended period. Because dimercaptosuccinic acid accumulates in the functioning renal cortex, the impaired renal cortex and space-occupying lesions are revealed as hypoactive areas (Fig 11).[10,63,65]

Differential or "split" renal function is calculated either by using the
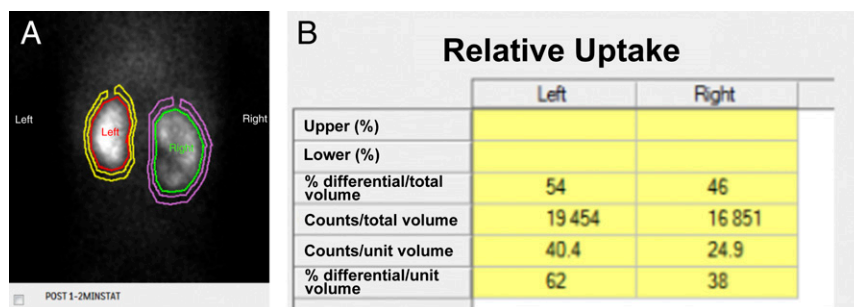

FIGURE 10

A, Nuclear medicine renal scan with ^{99m}Tc-MAG3 of a 13-month-old girl with bilateral UTD at birth. B, The study reveals decreased uptake by the right kidney, with a differential renal function of 46% for the right kidney and 54% for the left kidney.

number of counts produced from each kidney during the uptake phase after (contrast or radiotracer) injection or by using a graphical analysis technique (Rutland–Patlak model) and is expressed as a percentage of the sum of the right and left computed parameters. In subjects with normal renal function, the 95% confidence interval for the relative uptake of ^{99m}Tc-MAG3 ranges from 42% to 58%.[68] The spatial resolution (ie, the number of pixels used to reconstruct an image and, hence, a measure of the ability of the image to discriminate between 2 adjacent structures) of nuclear medicine studies is much lower (10 mm in plane resolution) than the spatial resolution of anatomic imaging modalities such as ultrasound (0.1 mm), CT (0.5 mm), or MRI (1 mm). Hence, in patients with dilated renal

calyces and dilated renal pelvis, the postprocessing analysis might not be truly representative of the area of functional interest (parenchyma only) but may also include the collecting system itself. Acknowledging a certain degree of inaccuracy, the renal size is determined from the pixel length and area of the whole kidney (Fig 10).[63,69]

Mercaptoacetyltriglycine renal scan has multiple advantages, most importantly, because there is extensive clinical experience. Additionally, the radiotracers are nonnephrotoxic and without risk of accumulation or deposition in the body.[63] Disadvantages of mercaptoacetyltriglycine renal scans include a lower spatial resolution and concern about the use of radiation. However, the usual radiation dose
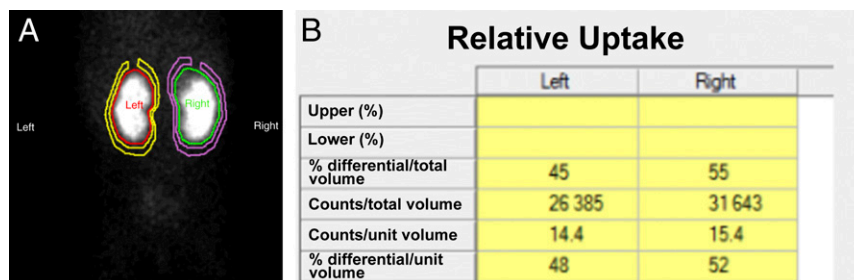

FIGURE 11

^{99m}Tc-DMSA renal scan in a 10-month-old girl with a history of right grade II and left grade III VUR and recurrent UTIs. A, Cortical defects on the upper pole of the right kidney and midportion of the left kidney. B, The differential renal function is 45% vs 55% for the left and right kidney, respectively.

represents <5% of the yearly radiation dose considered safe for radiation workers.[63,70] After 3 hours, >95% of ^{99m}Tc-MAG3 leaves the body in patients with normal kidney function, and patients can go to public places and use a bathroom without risk to exposing others to radiation.[63]

fMRU

fMRU provides a comprehensive morphologic and functional evaluation of the urinary tract in a radiation-free single examination with excellent spatial, contrast, and temporal resolution and is therefore becoming the test of choice in patients with complex anatomy. fMRU depicts detailed anatomy of the genitourinary system, serving as a presurgical road map with a high level of confidence because it provides a precontrast 3D reconstruction. As part of the protocol, patients receive IV hydration and diuretics (furosemide) before image acquisition for better resolution. Similarly, the bladder is and should be catheterized to reduce the confounding effect of difficulty voiding and/or VUR. For the functional part of the study, a gadolinium-based contrast agent is administered steadily and images are acquired dynamically over time. The important clinical, functional information obtained from analyzing contrast flow dynamics allows for some degree of confidence in differentiating obstructed from nonobstructed renal collecting systems (Figs 12 and Figs 13).[71] During the 8-minute high-resolution dynamic scan, the enhancement of the aorta, the kidneys, and, in most cases, the initial drainage flow of the urinary system is obtained. Postprocessing fMRU-specific software is required to obtain quantitative parameters as well as enhancement and excretion curves. The most widely used functional analysis software is a custom-made freeware known as
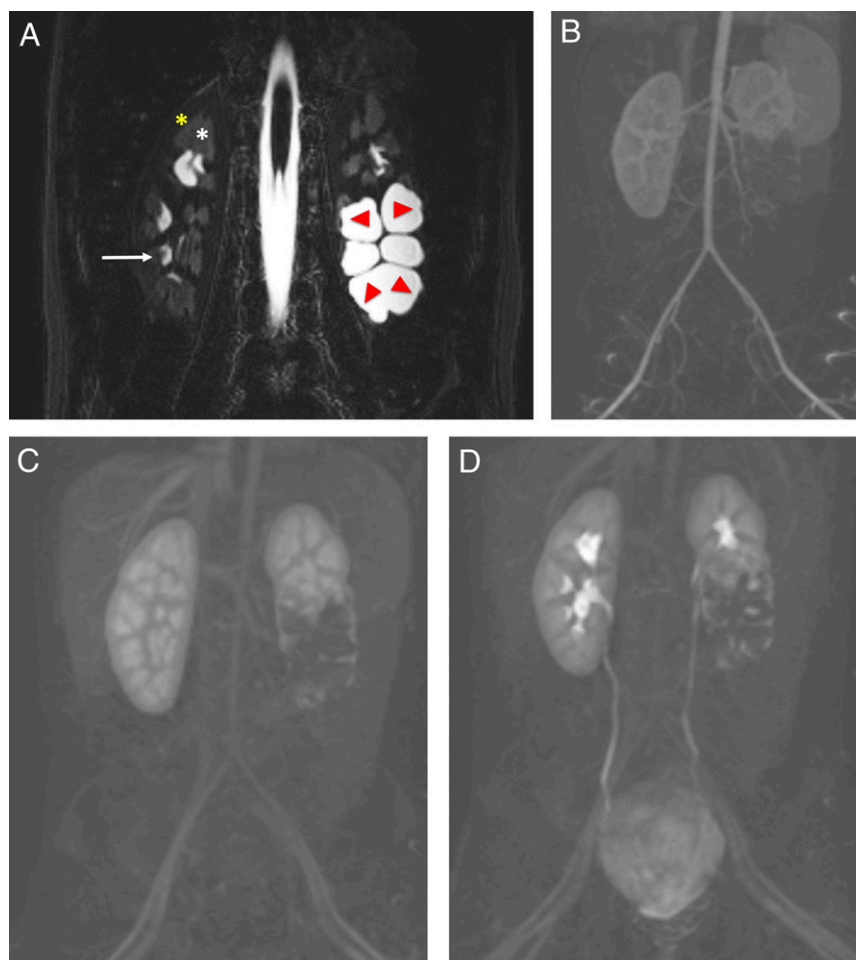

FIGURE 12

Renal anatomy as seen in MRU. A, Coronal fluid-sensitive (heavily T2-weighted) MR image reveals a normal right kidney with low-signal intensity of the cortex (yellow star), intermediate-signal intensity of the medulla (white star) and high intensity (urine) within the normal calyces (white arrow). The left kidney has a duplicated collecting system with markedly dilated central calyces in the lower pole, which is obstructed (red arrows). B–D, Coronal dynamic subtracted postcontrast T1-weighted MR images reveal the transit of contrast from the aorta and cortex, to the medullary renal parenchyma, and into the collecting system, including delineation of the normal ureters and bladder, which is normal in the right kidney and upper pole of the left kidney but incomplete and delayed of the abnormal left lower moiety.

CHOP-fMRU (www.chop-fmru.com).[72]

The enhancement and excretion curves are a display of the change of signal intensity over time and are calculated for the aorta, renal parenchyma, pelvis, and calyces with higher spatial resolution than nuclear medicine studies. Each curve represents the relative enhancement of the segmented region of interest over time from the baseline (ie, precontrast signal). The excretion curve is focused on the change of signal intensity generated by the contrast accumulation in the collecting system. It is important to note that an abnormally prolonged renal transit time (the time needed for the contrast agent to reach the ureter below the level of the lower pole of the kidney) does not necessarily discriminate between ureteropelvic obstruction and the pooling of the contrast agent in a dilated renal pelvis.[72] Imaging with the patient in prone position helps to mitigate this

Features / Imaging modality	Preparation S/H/UC[a]	Duration (min)	Anatomy detail (0–5 stars)	Function evaluation (0-5 stars)	Drainage obstruction evaluation (ureter seen? Yes or no)	Common clinical indications	Ionizing radiation (yes or no)	Nephrotoxic (yes or no)	Relative cost
Plain films	None	5			No	• Nephrolithiasis • Urolithiasis	⚠ (yes)	N/A	$
Conventional ultrasound	None	30	★★★	★	Yes[b]	• UTD • CAKUT • Nephrolithiasis • Cysts • Reflux	No	N/A	$
Doppler ultrasound	None	45	★★★	★★	No	• Vasculature stenosis • Perfusion	No	N/A	$$
CEUS	None	45	★★★★	★★★	Yes[b]	• UTD • CAKUT (cystic disease) • Perfusion • Masses	No	No	$$
CeVUS	None	30	★★★★		Yes	• Reflux • Urethral anomalies	No	No	$$
VCUG	UC	30	★★★★		Yes	• Reflux • Urethral anomalies	⚠	No	$$
CT urography	None	15	★★★★	★★★	Yes	• GU trauma • Obstructive uropathy • Calyceal diverticula	⚠	Yes	$$$
Contrast MRI	Sedation	60	★★★★★	★★★	Yes	• CAKUT • Masses	No	No[c]	$$$$
MR urography	S/H/UC	60	★★★★★	★★★★★[d]	Yes	• Obstructive uropathy • Reflux • Complex GU anomalies	No	No[c]	$$$$
Mercaptoace-tyltriglycine diuretic renography	Sedation and UC	90	★★	★★★★[d]	Yes	• Obstructive uropathy	⚠	No	$$$
DMSA scan	Sedation	30	★★★	★★★★[d]	No	• Renal scarring • MCDK	⚠	No	$$$

FIGURE 13

Summary of renal imaging modalities, indications, ionizing radiation risk, nephrotoxic effect, and estimated cost associated. [a] S/H/UC refers to the need of sedation, IV hydration, and a urinary catheter (UC) for the completion of the study. In general, sedation for any of these imaging tests is only needed in patients >6 months and <5 years of age. [b] Not able to visualize dilated ureter all the time. [c] Risk of NSF in patients with abnormal renal function is thought to be lower with a newer generation of macrocyclic gadolinium-based contrast agents (eg, gadobutrol, gadoteridol, and gadoterate). [d] Split function. DMSA, dimercaptosuccinic acid; GU, genitourinary; MCDK, multycystic dysplastic kidney; N/A, not applicable.

effect. Delayed imaging can be obtained to try to demonstrate contrast in the ureter and/or bladder.[72]

fMRU also has some ancillary disadvantages, including the need for sedation or anesthesia for younger children, cost and availability of an MR scan, and the potential adverse events related to gadolinium contrast agents. Nephrogenic systemic fibrosis (NSF) has been described with the use of an older generation of gadolinium-based contrast agents in patients with severe renal failure, which limits its use in patients with advanced CKD. However, the risk of NSF is thought to be lower with newer macrocyclic

gadolinium-based agents (eg, gadobutrol, gadoteridol, and gadoterate).[73] There may also be a risk of gadolinium deposition throughout the body, but further study is required to determine the clinical significance, if any.[74,75]

CONCLUSIONS

With new imaging technologies, we attempt to achieve higher imaging resolution, reduce imaging time, and minimize radiation exposure. The ultimate goal is to fully characterize CAKUT in young children with a higher degree of accuracy while providing noninvasive prognostic information in patients at risk for developing CKD.[76,77] It is important to continue to develop imaging biomarkers as tools to detect progression of renal disease. Clinicians can use this review for reference when navigating different imaging modalities (Fig 13) as part of the team caring for patients with suspected or known renal disease. To summarize, (1) CEUS is most promising in evaluating focal renal disease, with a comparably favorable safety profile of the contrast agent; (2) CeVUS has advantages over VCUG, with higher sensitivity for the detection of clinically significant VUR; (3) fMRU provides comprehensive functional information with improved anatomic information when compared with nuclear medicine renograms; and (4) 3D-printed models are increasingly used for training and surgical planning in the kidney and urinary system. Familiarity with these technologies will allow for easier adoption and wider dissemination of knowledge as, with ongoing research efforts, we attempt to shed light on the natural course of disease and guide therapies with safer and more patient-centered imaging strategies.

ABBREVIATIONS

3D: three-dimensional
3DUS: three-dimensional ultrasound
^{99m}Tc-DMSA: ^{99m}Tc-labeled dimercaptosuccinic acid
^{99m}Tc-MAG3: ^{99m}Tc-labeled mercaptoacetyltriglycine
CAKUT: congenital anomalies of the kidney and urinary tract
CEUS: contrast-enhanced ultrasound
CeVUS: contrast-enhanced voiding urosonography
CKD: chronic kidney disease
CT: computed tomography
DTPA: diethylenetriaminepentaacetic acid
fMRU: functional magnetic resonance urography
IV: intravenous
MR: magnetic resonance
MRU: magnetic resonance urography
NSF: nephrogenic systemic fibrosis
PC-AKI: postcontrast acute kidney injury
RBUS: renal and bladder ultrasound
UCA: ultrasound contrast agent
UTD: urinary tract dilation
UTI: urinary tract infection
VCUG: voiding cystourethrography
VUR: vesicoureteral reflux

REFERENCES

1. Ingelfinger JR, Kalantar-Zadeh K, Schaefer F; World Kidney Day Steering Committee. Averting the legacy of kidney disease–focus on childhood. *Kidney Int.* 2016;89(3):512–518

2. Weaver DJ Jr., Somers MJG, Martz K, Mitsnefes MM. Clinical outcomes and survival in pediatric patients initiating chronic dialysis: a report of the NAPRTCS registry. *Pediatr Nephrol.* 2017;32(12):2319–2330

3. Moran SM, Myers BD. Course of acute renal failure studied by a model of creatinine kinetics. *Kidney Int.* 1985; 27(6):928–937

4. Stoll C, Dott B, Alembik Y, Roth MP. Associated nonurinary congenital anomalies among infants with congenital anomalies of kidney and urinary tract (CAKUT). *Eur J Med Genet.* 2014;57(7):322–328

5. Queisser-Luft A, Stolz G, Wiesel A, Schlaefer K, Spranger J. Malformations in newborn: results based on 30,940 infants and fetuses from the Mainz congenital birth defect monitoring system (1990-1998). *Arch Gynecol Obstet.* 2002;266(3):163–167

6. Feldenberg R, Beck A. Congenital diseases of the kidneys: prognosis and treatments. *Neoreviews.* 2017;18(6): e345–e356

7. Poudel A, Afshan S, Dixit M. Congenital anomalies of the kidney and urinary tract. *Neoreviews.* 2016;17(1):e18–e27

8. Nguyen HT, Benson CB, Bromley B, et al. Multidisciplinary consensus on the classification of prenatal and postnatal urinary tract dilation (UTD classification system). *J Pediatr Urol.* 2014;10(6):982–998

9. Kaspar CDW, Lo M, Bunchman TE, Xiao N. The antenatal urinary tract dilation classification system accurately predicts severity of kidney and urinary tract abnormalities. *J Pediatr Urol.* 2017;13(5):485.e1-485.e7

10. Mujoomdar M, Russell E, Dionne F, et al. *Optimizing Health System Use of Medical Isotopes and Other Imaging Modalities.* Ottawa, Canada: Canadian Agency for Drugs and Technologies in Health; 2012

11. Perez-Brayfield MR, Kirsch AJ, Jones RA, Grattan-Smith JD. A prospective study comparing ultrasound, nuclear scintigraphy and dynamic contrast enhanced magnetic resonance imaging in the evaluation of hydronephrosis. *J Urol.* 2003;170(4, pt 1):1330–1334

12. Peters CA. Urinary tract obstruction in children. *J Urol.* 1995;154(5): 1874–1883–1884

13. Ismail A, Elkholy A, Zaghmout O, et al. Postnatal management of antenatally diagnosed ureteropelvic junction obstruction. *J Pediatr Urol.* 2006;2(3): 163–168

14. Dunnick NR, Sandler CM, Newhouse JH. Anatomy and embryology. In: *Textbook of Uroradiology*, 5th ed. Philadelphia, PA: Lippincott Williams & Wilkins; 2013: 1–12

15. Riccabona M. Potential role of 3DUS in infants and children. *Pediatr Radiol*. 2011;41(suppl 1):S228–S237

16. Riccabona M. Modern pediatric ultrasound: potential applications and clinical significance. A review. *Clin Imaging*. 2006;30(2):77–86

17. Riccabona M. Basics, principles, techniques and modern methods in paediatric ultrasonography. *Eur J Radiol*. 2014;83(9):1487–1494

18. Bartram U, Darge K. Harmonic versus conventional ultrasound imaging of the urinary tract in children. *Pediatr Radiol*. 2005;35(7):655–660

19. Riccabona M, Fritz GA, Schöllnast H, Schwarz T, Deutschmann MJ, Mache CJ. Hydronephrotic kidney: pediatric three-dimensional US for relative renal size assessment—initial experience. *Radiology*. 2005;236(1): 276–283

20. Cerrolaza JJ, Otero H, Yao P, et al. Semi-automatic assessment of pediatric hydronephrosis severity in 3D ultrasound. In: Proceedings from SPIE Medical Imaging 2016: Computer-Aided Diagnosis; February 27–March 3, 2016; San Diego, CA

21. Riccabona M, Nelson TR, Pretorius DH, Davidson TE. Distance and volume measurement using three-dimensional ultrasonography. *J Ultrasound Med*. 1995;14(12):881–886

22. Treece G, Prager R, Gee A, Berman L. 3D ultrasound measurement of large organ volume. *Med Image Anal*. 2001; 5(1):41–54

23. Cosgrove D, Piscaglia F, Bamber J, et al; EFSUMB. EFSUMB guidelines and recommendations on the clinical use of ultrasound elastography part 2: clinical applications. *Ultraschall in der Medizin*. 2013;34(3):238–253

24. Bamber J, Cosgrove D, Dietrich CF, et al. EFSUMB guidelines and recommendations on the clinical use of ultrasound elastography. Part 1: basic principles and technology. *Ultraschall Med*. 2013;34(2):169–184

25. Kummer S, Sagir A, Pandey S, et al. Liver fibrosis in recessive multicystic kidney diseases: transient elastography for early detection. *Pediatr Nephrol*. 2011;26(5):725–731

26. Wang L. Applications of acoustic radiation force impulse quantification in chronic kidney disease: a review. *Ultrasonography*. 2016;35(4):302–308

27. Cerrolaza JJ, Peters CA, Martin AD, Myers E, Safdar N, Linguraru MG. Quantitative ultrasound for measuring obstructive severity in children with hydronephrosis. *J Urol*. 2016;195(4, pt 1):1093–1099

28. McArthur C, Baxter GM. Current and potential renal applications of contrast-enhanced ultrasound. *Clin Radiol*. 2012; 67(9):909–922

29. Pan FS, Liu M, Luo J, et al. Transplant renal artery stenosis: evaluation with contrast-enhanced ultrasound. *Eur J Radiol*. 2017;90:42–49

30. Barr RG, Peterson C, Hindi A. Evaluation of indeterminate renal masses with contrast-enhanced US: a diagnostic performance study. *Radiology*. 2014; 271(1):133–142

31. Paudice N, Zanazzi M, Agostini S, et al. Contrast-enhanced ultrasound assessment of complex cystic lesions in renal transplant recipients with acquired cystic kidney disease: preliminary experience. *Transplant Proc*. 2012;44(7):1928–1929

32. Mueller-Peltzer K, Negrão de Figueiredo G, Fischereder M, Habicht A, Rübenthaler J, Clevert DA. Contrast-enhanced ultrasound (CEUS) as a new technique to characterize suspected renal transplant malignancies in renal transplant patients in comparison to standard imaging modalities. *Clin Hemorheol Microcirc*. 2018;69(1–2): 69–75

33. Benozzi L, Cappelli G, Granito M, et al. Contrast-enhanced sonography in early kidney graft dysfunction. *Transplant Proc*. 2009;41(4):1214–1215

34. Fernandez CP, Ripolles T, Martinez MJ, Blay J, Pallardó L, Gavela E. Diagnosis of acute cortical necrosis in renal transplantation by contrast-enhanced ultrasound: a preliminary experience. *Ultraschall Med*. 2013;34(4):340–344

35. Mori G, Granito M, Favali D, Cappelli G. Long-term prognostic impact of contrast-enhanced ultrasound and power doppler in renal transplantation. *Transplant Proc*. 2015;47(7):2139–2141

36. Mueller-Peltzer K, Negrão de Figueiredo G, Fischereder M, Habicht A, Rübenthaler J, Clevert DA. Vascular rejection in renal transplant: diagnostic value of contrast-enhanced ultrasound (CEUS) compared to biopsy. *Clin Hemorheol Microcirc*. 2018;69(1–2): 77–82

37. Yang WQ, Mou S, Xu Y, Xu L, Li FH, Li HL. Quantitative parameters of contrast-enhanced ultrasonography for assessment of renal pathology: a preliminary study in chronic kidney disease. *Clin Hemorheol Microcirc*. 2018;68(1):71–82

38. Yang C, Wu S, Yang P, et al. Prediction of renal allograft chronic rejection using a model based on contrast-enhanced ultrasonography. *Microcirculation*. 2019;26(6):e12544

39. American College of Radiology. ACR–SPR practice parameter for the performance of fluoroscopic and sonographic voiding cystourethrography in children. 2016. Available at: https://www.acr.org/-/media/ACR/Files/Practice-Parameters/VoidingCysto.pdf. Accessed November 15, 2018

40. Papadopoulou F, Ntoulia A, Siomou E, Darge K. Contrast-enhanced voiding urosonography with intravesical administration of a second-generation ultrasound contrast agent for diagnosis of vesicoureteral reflux: prospective evaluation of contrast safety in 1,010 children. *Pediatr Radiol*. 2014;44(6): 719–728

41. Riccabona M, Vivier PH, Ntoulia A, et al; ESPR Uroradiology Task Force. ESPR uroradiology task force imaging recommendations in paediatric uroradiology, part VII: standardised terminology, impact of existing recommendations, and update on contrast-enhanced ultrasound of the paediatric urogenital tract. *Pediatr Radiol*. 2014;44(11):1478–1484

42. Papadopoulou F, Anthopoulou A, Siomou E, Efremidis S, Tsamboulas C, Darge K. Harmonic voiding urosonography with a second-generation contrast agent for

the diagnosis of vesicoureteral reflux. *Pediatr Radiol.* 2009;39(3):239–244

43. Darge K. Voiding urosonography with US contrast agents for the diagnosis of vesicoureteric reflux in children. II. Comparison with radiological examinations. *Pediatr Radiol.* 2008; 38(1):54–63–127

44. Duran C, Beltrán VP, González A, Gómez C, Riego JD. Contrast-enhanced voiding urosonography for vesicoureteral reflux diagnosis in children. *Radiographics.* 2017;37(6):1854–1869

45. Woźniak MM, Osemlak P, Pawelec A, et al. Intraoperative contrast-enhanced urosonography during endoscopic treatment of vesicoureteral reflux in children. *Pediatr Radiol.* 2014;44(9): 1093–1100

46. Mitsouras D, Liacouras P, Imanzadeh A, et al. Medical 3D printing for the radiologist. *Radiographics.* 2015;35(7): 1965–1988

47. Martelli N, Serrano C, van den Brink H, et al. Advantages and disadvantages of 3-dimensional printing in surgery: a systematic review. *Surgery.* 2016; 159(6):1485–1500

48. Jones DB, Sung R, Weinberg C, Korelitz T, Andrews R. Three-dimensional modeling may improve surgical education and clinical practice. *Surg Innov.* 2016;23(2):189–195

49. Dwivedi DK, Chatzinoff Y, Zhang Y, et al. Development of a patient-specific tumor mold using magnetic resonance imaging and 3-dimensional printing technology for targeted tissue procurement and radiomics analysis of renal masses. *Urology.* 2018;112: 209–214

50. Silberstein JL, Maddox MM, Dorsey P, Feibus A, Thomas R, Lee BR. Physical models of renal malignancies using standard cross-sectional imaging and 3-dimensional printers: a pilot study. *Urology.* 2014;84(2):268–272

51. Bernhard JC, Isotani S, Matsugasumi T, et al. Personalized 3D printed model of kidney and tumor anatomy: a useful tool for patient education. *World J Urol.* 2016;34(3):337–345

52. Cone EB, Dalton SS, Van Noord M, Tracy ET, Rice HE, Routh JC. Biomarkers for Wilms tumor: a systematic review. *J Urol.* 2016;196(5):1530–1535

53. Tricard T, Lacreuse I, Louis V, et al. Is nephron-sparing surgery relevant for unilateral Wilms tumors?[in French]. *Arch Pediatr.* 2017;24(7):650–658

54. Vernuccio F, Meyer M, Mileto A, Marin D. Use of dual-energy computed tomography for evaluation of genitourinary diseases. *Urol Clin North Am.* 2018;45(3):297–310

55. Raman SP, Fishman EK. Upper and lower tract urothelial imaging using computed tomography urography. *Urol Clin North Am.* 2018;45(3):389–405

56. Dillman JR, Rigsby CK, Iyer RS, et al; Expert Panel on Pediatric Imaging. ACR Appropriateness Criteria® hematuria-child. *J Am Coll Radiol.* 2018;15(suppl 5):S91–S103

57. Van Der Molen AJ, Cowan NC, Mueller-Lisse UG, Nolte-Ernsting CC, Takahashi S, Cohan RH; CT Urography Working Group of the European Society of Urogenital Radiology (ESUR). CT urography: definition, indications and techniques. A guideline for clinical practice. *Eur Radiol.* 2008;18(1):4–17

58. Callahan MJ, Servaes S, Lee EY, Towbin AJ, Westra SJ, Frush DP. Practice patterns for the use of iodinated i.v. contrast media for pediatric CT studies: a survey of the Society for Pediatric Radiology. *AJR Am J Roentgenol.* 2014; 202(4):872–879

59. Beckett KR, Moriarity AK, Langer JM. Safe use of contrast media: what the radiologist needs to know. *Radiographics.* 2015;35(6):1738–1750

60. American College of Radiology Committee on Drugs and Contrast Media. ACR manual on contrast media. Version 10.3. 2018. Available at: https://www.acr.org/-/media/ACR/Files/Clinical-Resources/Contrast_Media.pdf. Accessed November 15, 2018

61. Cantais A, Hammouda Z, Mory O, et al. Incidence of contrast-induced acute kidney injury in a pediatric setting: a cohort study. *Pediatr Nephrol.* 2016; 31(8):1355–1362

62. Hinson JS, Ehmann MR, Fine DM, et al. Risk of acute kidney injury after intravenous contrast media administration. *Ann Emerg Med.* 2017; 69(5):577–586.e4

63. Taylor AT. Radionuclides in nephrourology, part 1: radiopharmaceuticals, quality control, and quantitative indices. *J Nucl Med.* 2014;55(4):608–615

64. Taylor A Jr., Nally JV. Clinical applications of renal scintigraphy. *AJR Am J Roentgenol.* 1995;164(1):31–41

65. Ziessman HA, O'Malley JP, Thrall JH. Genitourinary system. In: Thrall JH, Fahey FH. ed. *Nuclear Medicine: The Requisites.* 4th ed. Philadelphia, PA: Elsevier Inc; 2014:168–203

66. Strauss BS, Blaufox MD. Estimation of residual urine and urine flow rates without urethral catheterization. *J Nucl Med.* 1970;11(2):81–84

67. Prigent A, Cosgriff P, Gates GF, et al. Consensus report on quality control of quantitative measurements of renal function obtained from the renogram: International Consensus Committee from the Scientific Committee of Radionuclides in Nephrourology. *Semin Nucl Med.* 1999;29(2):146–159

68. Esteves FP, Taylor A, Manatunga A, Folks RD, Krishnan M, Garcia EV. 99mTc-MAG3 renography: normal values for MAG3 clearance and curve parameters, excretory parameters, and residual urine volume. *AJR Am J Roentgenol.* 2006;187(6):W610–W617

69. Durand E, Chaumet-Riffaud P, Grenier N. Functional renal imaging: new trends in radiology and nuclear medicine. *Semin Nucl Med.* 2011;41(1):61–72

70. Stabin M, Taylor A Jr., Eshima D, Wooter W. Radiation dosimetry for technetium-99m-MAG3, technetium-99m-DTPA, and iodine-131-OIH based on human biodistribution studies. *J Nucl Med.* 1992;33(1):33–40

71. Jones RA, Perez-Brayfield MR, Kirsch AJ, Grattan-Smith JD. Renal transit time with MR urography in children. *Radiology.* 2004;233(1):41–50

72. Khrichenko D, Darge K. Functional analysis in MR urography - made simple. *Pediatr Radiol.* 2010;40(2): 182–199

73. Prybylski JP, Jay M. The impact of excess ligand on the retention of nonionic, linear gadolinium-based contrast agents in patients with various levels of renal dysfunction: a review and simulation analysis. *Adv Chronic Kidney Dis.* 2017;24(3):176–182

74. Holowka S, Shroff M, Chavhan GB. Use and safety of gadolinium based contrast agents in pediatric MR imaging. *Indian J Pediatr.* 2019;86(10): 961–966

75. Gulani V, Calamante F, Shellock FG, Kanal E, Reeder SB; International Society for Magnetic Resonance in Medicine. Gadolinium deposition in the brain: summary of evidence and recommendations. *Lancet Neurol.* 2017; 16(7):564–570

76. Renkema KY, Winyard PJ, Skovorodkin IN, et al; EUCAKUT consortium. Novel perspectives for investigating congenital anomalies of the kidney and urinary tract (CAKUT). *Nephrol Dial Transplant.* 2011;26(12): 3843–3851

77. Chow JS, Koning JL, Back SJ, Nguyen HT, Phelps A, Darge K. Classification of pediatric urinary tract dilation: the new language. *Pediatr Radiol.* 2017;47(9): 1109–1115